$Cu_2ZnGe(S_{1-x}Se_x)_4$ – the challenge to synthesize single phase material

Sara Niedenzu[1,2,*], Galina Gurieva[1], and Susan Schorr[1,2]

[1]Helmholtz-Zentrum Berlin für Materialien und Energie, Berlin, Hahn-Meitner-Platz 1, Germany

[2]Freie Universität Berlin, Berlin, Malteserstr. 74, Germany

E-Mail addresses: sara.niedenzu@helmholtz-berlin.de, galina.gurieva@helmholtz-berlin.de, susan.schorr@helmholtz-berlin.de

*corresponding author: Sara Niedenzu, E-Mail address: sara.niedenzu@helmholtz-berlin.de, Phone number: +49 30 8062 43237,

present address: Helmholtz-Zentrum Berlin für Materialien und Energie, Hahn-Meitner-Platz 1, 14109 Berlin

Abstract — The variation of the band gap energy in $Cu_2ZnGeSe_4$ and Cu_2ZnGeS_4 from 1.4 eV to 1.7 eV, which is controlled by different S/(S+Se) ratios renders the $Cu_2ZnGe(S_{1-x}Se_x)_4$ solid solution an interesting material for the application in multi-junction solar cells. Nevertheless, this system has a certain complexity due to the existence of different polymorphs. $Cu_2ZnGeSe_4$ crystallizes in the tetragonal kesterite type structure, whereas Cu_2ZnGeS_4 may crystallize in the tetragonal stannite or the orthorhombic wurtz-stannite type structure, respectively.

To gain deeper insights into this complex system a systematic study of the solid solution series $Cu_2ZnGe(S_{1-x}Se_x)_4$ was performed using polycrystalline material prepared by solid state reaction. The chemical analysis performed by wavelength dispersive X-ray spectroscopy showed remarkable inhomogeneities with different quaternary phases co-existing within one sample. Additionally, a wide variety of binary and ternary secondary phases as well as elemental Ge was observed. The variety of secondary phases is higher in S-rich samples than in Se-rich samples of the solid solution. Thus, synthesis of $Cu_2ZnGe(S_{1-x}Se_x)_4$ mixed crystals with off-stoichiometric composition is readily accompanied by the formation of various secondary phases making it a difficult task to obtain single phase material.

Keywords — Copper zinc germanium selenide; Copper zinc germanium sulfide; Polycrystalline powders; Solid state reaction; Wavelength dispersive X-ray spectroscopy; Chalcogenides; Secondary phases.

1. INTRODUCTION

The quaternary chalcogenide semiconductors Cu_2-B^{II}-C^{IV}-X_4 (B^{II}-Zn; C^{IV}-Ge, X-S, Se) contain only earth abundant, non-toxic elements and have drawn wide attention for their potential applications in the fields of photovoltaics and thermoelectrics [1,2]. In the last years much attention has been paid to Cu_2ZnSnS_4 (CZTS)

and $Cu_2ZnSnSe_4$ (CZTSe) for the usage in solar cell devices, and various approaches has been attempted to optimize their opto-electronic properties [1,3,4,5,6]. When, for instance, alloyed with Ge it is assumed that the device performance of CZTSSe thin film solar cells is significantly improved [1]. Cation substitution (Sn ↔ Ge) but also different anion ratios (S – Se) enable the tuning of the optical band gap and offers new opportunities in the development of highly efficient CZTGSSe based photovoltaic devices [1,3]. The variation of the band gap energy in $Cu_2ZnGeSe_4$ and Cu_2ZnGeS_4 from 1.4 eV to 1.7 eV and its control by different S/(S+Se) anion ratios makes the $Cu_2ZnGe(S_{1-x}Se_x)_4$ solid solution to an interesting candidate for top cells in multi-junction solar cells [7].

The crystal structure and possibly present point defects influence the electronic and optical properties of a material to a high degree. Insights into this structure-property relationship is key for the design of well-performing materials as it requires an understanding of the crystallographic materials properties. Experimental and theoretical studies show that $Cu_2ZnGeSe_4$ crystallizes in the kesterite type structure (space group $I\bar{4}$) [8, 9], which is also predicted to be the ground state structure for this material [10]. The experimental results demonstrating that $Cu_2ZnGeSe_4$ adopts the kesterite type structure are based on neutron diffraction data [9]. According to powder X-ray diffraction, Cu_2ZnGeS_4 is reported to crystallize in the tetragonal stannite type structure (space group $I\bar{4}2m$) at room temperature [11,12] and in the orthorhombic wurtz-stannite type structure (space group $Pmn2_1$) at high temperatures [11]. The phase transition from the tetragonal to the orthorhombic structure is reported to occur between 790 °C [11] and 810 °C [12]. To get a detailed view into this complex system we have performed a systematic study comprising synthesis and characterization of the solid solution $Cu_2ZnGe(S_{1-x}Se_x)_4$ over the full composition range from x = 0 – 1.

2. Experimental

Polycrystalline powder samples of the $Cu_2ZnGe(S_{1-x}Se_x)_4$ solid solution were synthesized by solid state reaction from the pure (5N) elements Cu, Zn, Ge, S, and Se. The weighed elements were placed in a graphite

boat and sealed in evacuated silica tubes which, in turn, were placed in a tubular one-zone furnace. For the reaction step the samples were heated up to 750 °C (x = 0 – 0.2), 730 °C (x = 0.3 – 0.5), 720 °C (x = 0.6 – 0.8) and 700 °C (x = 0.9 – 1) using a heating rate of 10 K/h (Tab. 1). The maximum temperatures were hold for 300 h. The different temperatures were chosen to stay below the melting point as well as below the reported structural phase transition of the quaternary compound, thus, eventually resulting in different maximum temperatures depending on the S:Se anion ratio. The melting temperatures for Cu_2ZnGeS_4 and $Cu_2ZnGeSe_4$ are 969 °C [12] and 890 °C [13], respectively. The structural phase transition of Cu_2ZnGeS_4 is reported to occur between 790 °C [11] and 810 °C [12]. Intermediate steps at 250 °C (48 h), 450 °C (48 h), and 650 °C (48 h) were introduced for balancing between reaction velocity and, otherwisely, a too rapidly increasing partial pressure of S and Se. The samples were cooled down to room temperature with a cooling rate of 10 K/h. In a subsequent step the samples were homogenized by grinding them in an agate mortar and by pressing the obtained powder into pellets. The pellets were annealed in evacuated silica tubes in the tubular one-zone furnace for 300 h at the same temperatures as chosen for the reaction step. While the heating rate for the annealing step has now been increased to 50 K/h, the cooling again was performed using 10 K/h.

The chemical homogeneity and chemical composition of the synthesized polycrystalline powders were proven by quantitative wavelength dispersive X-ray spectroscopy (WDX) using an electron microprobe of the type JEOL JXA 8200 Superprobe. The quantitative element analysis includes an error of 2 %. 35 grains per sample were measured with 10 measurement points each. However, as there are different kinds of quaternary phases present in each sample, the number of grains that could been used for averaging the composition of each quaternary phase in a sample varies between 5 and 20. The elemental distribution within specific grains in the synthesized polycrystalline powders were analyzed by energy dispersive X-ray analysis (EDX) using a scanning electron microscope (SEM) of the type LEO Gemini 1530. The qualitative element mapping was performed in the high-resolution mode with an aperture size of 120 µm and an acceleration voltage of 10 kV.

3. RESULTS AND DISCUSSION

3.1 OFF-STOICHIOMETRY

Back scattered electron (BSE) images (Fig. 1) taken at the electron microprobe show that the samples from the solid solution are very inhomogeneous, which can be concluded owing to the different grey coloring of the grains. Furthermore, it can be observed that the $Cu_2ZnGeSe_4$ (x=1) sample and the Se-rich mixed crystals appear less inhomogeneous than the Cu_2ZnGeS_4 (x=0) sample and the S-rich mixed crystals. Chemical analysis revealed a broad range of secondary phases, and, with the exception of two samples, the presence of more than one quaternary phase (Tab. 2).

The samples containing the single quaternary phase are the endmember Cu_2ZnGeS_4 and the S-rich mixed crystal $Cu_2ZnGe(S_{1-x}Se_x)_4$ with x = 0.1. Both of them are Cu-rich and Zn-poor (Fig. 2). The other mixed crystals (x = 0.2 – 1) of the $Cu_2ZnGe(S_{1-x}Se_x)_4$ series contain more than one quaternary phase. The number of quaternary phases present in a sample ranges between two and five, and the chemical analysis suggests that the amount of quaternary phases tends to be higher in the Se-rich than in the S-rich ones. (Fig. 2). The quaternary phases within a sample show strong variations in the chemical compositions and, thus, plot over a wide range in the cation-ratio plot (Fig. 2). Each of these inhomogeneous samples show quaternary phases around the transition from the Cu-poor/Zn-poor to the Cu-rich/Zn-poor regime close to the stoichiometric point (Fig. 2). In addition, at least one quaternary phase in each of these samples plots very far off-stoichiometric in the Cu-poor/Zn-rich region (Fig. 2). This means that slightly Cu-rich/Zn-poor or slightly Cu-poor/Zn-poor quaternary phases always go along with at least one far off-stoichiometric Cu-poor/Zn-rich quaternary phase. The deviations from stoichiometry in the $Cu_2ZnGe(S_{1-x}Se_x)_4$ mixed crystals can be explained by the presence of secondary phases as well as by the volatility of Ge and S. The amount, the variety and chemical compositions of the secondary phases as well as the amount of volatile elements involved are decisive to which specific region of the cation-ratio plot the quaternary phases belong.

3.2 SECONDARY PHASES

In all of the samples Zn(S,Se) has been observed as a secondary phase while in the samples with a S-rich composition (x = 0.0 – 0.4) a broader range of secondary phases is present. In these samples also copper sulfides and selenides can be observed in which Cu appears in different oxidation states (Cu(S,Se) and Cu_2(S,Se)). Cu is partially substituted by Ge in all copper selenides. Apart from that also grains of pure Ge, which have not been reacted during the synthesis, are present in the S-rich mixed crystals (x = 0.1 – 0.3). The grain size of the binaries Zn(S,Se), Cu(S,Se), Cu_2(S,Se) as well as the pure Ge have the same size as the grains of the quaternary phases (Fig. 1). Ge is not only present as single grains, but also occurs at the rims of secondary phases like Cu(S,Se) (Fig. 3).

In addition to that a further ternary secondary phase has been observed in five samples of the $Cu_2ZnGe(S_{1-x}Se_x)_4$ solid solution (x = 0.1, 0.3, 0.4, 0.7, 0.8). With reference to its equal occurrence over the entire solid solution its formation appears to be independent from the anion ratio. The chemical composition of the ternary phase was determined as Cu_8GeSe_6 and Cu_8GeS_6, respectively, belonging to the family of argyrodite type compounds. Their melting temperatures are at 810 °C and 980 °C degree [14]. The Cu_8GeS_6-Cu_8GeSe_6 system is assumed to be the quasi-stable section of the corresponding quaternary system [14]. Both phases Cu_8GeS_6 and Cu_8GeSe_6 start to be present at lower temperatures and there is a polymorphic transition at 57 °C resulting in low-temperature (LT)- and high-temperature (HT)-modifications which show different crystal structures [14]. The LT-modification of Cu_8GeS_6 crystallizes in an orthorhombic structure with the space group $Pmn2_1$ [14,15], whereas the HT-modification crystallizes in a cubic crystal structure with the space group $F\bar{4}3m$ [14]. In case of Cu_8GeSe_6, the LT-modification crystallizes in a hexagonal crystal structure with the space group $P6_3mcm$ and the HT-modification in a cubic crystal structure (space group $F\bar{4}3m$) [14]. Since the melting temperatures of these phases are higher than the synthesis temperature applied for the solid solution series

which is between 700 °C and 750 °C, it is likely to happen that these phases may co-exist in the polycrystalline powder samples.

3.3 VOLATILITY OF GE AND S

The shift off the stoichiometric point (Fig. 2) can also be explained by the loss in Ge due to its volatility. Hence, difficulties in controlling this loss in Ge may also explain the widespread cation ratios in the mixed crystals of the $Cu_2ZnGe(S_{1-x}Se_x)_4$ series (Fig. 2). The loss in Ge during the synthesis has already been observed in polycrystalline powders of the end member $Cu_2ZnGeSe_4$ [9]. In addition to that, the low evaporation temperature of S and, hence, the loss of S during the sample preparation by sealing the ampoules may be a reason that the metals did not completely react, eventually explaining why elemental Ge partly remains in the powder samples. This could also explain why elemental Ge is found only in samples with higher S/(S+Se) ratios.

4. CONCLUSIONS

Polycrystalline powder material of the solid solution $Cu_2ZnGe(S_{1-x}Se_x)_4$ over the whole compositional range was synthesized by solid state reaction. The chemical analysis of the polycrystalline powders was performed quantitatively by WDX spectroscopy using an electron microprobe analysis system. All samples show more than one quaternary phase, except for two samples – Cu_2ZnGeS_4 and $Cu_2ZnGe(S_{1-x}Se_x)_4$ with x = 0.1. The quaternary phases vary tremendously in their chemical compositions within one sample and range from Cu-poor/Zn-poor as well as Cu-rich/Zn-poor to Cu-poor/Zn-rich compositions. Additionally, secondary phases like Zn(S,Se), copper selenides along with substitutional Ge, argyrodites as well as elemental metals like Ge have formed. Whereas in all samples of the solid solution Zn(S,Se) is present, the variety of secondary phases generally tends to increase towards S-rich samples of the solid solution $Cu_2ZnGe(S_{1-x}Se_x)_4$. In the Se-rich polycrystalline powders only Zn(S,Se) and $Cu_8Ge(S,Se)_6$ has been observed, while in S-rich polycrystalline

powders Cu(S,Se), Cu_2(S,Se) and elemental Ge is present in addition to Zn(S,Se) and $Cu_8Ge(S,Se)_6$. The presence of secondary phases as well as the off-stoichiometry of the quaternary phases are the two major problems for this solid solution. The reasons for that might be the volatility of Ge and S as well as the temperature dependent structural phase transition. To overcome these problems we suggest different possible solutions for further syntheses. By changing the temperature profile in terms of using higher temperatures, the amount of different structural phases as well as the amount of the argyrodite type secondary phases might be reduced. The incomplete reaction and, thus, the segregation of Ge might potentially be prevented employing fine-grained Ge powder to facilitate the reaction, instead of the rather large metal pieces. Also through a further annealing, the amount of secondary phases as well as the off-stoichiometry of the quaternary phases might be reduced. In addition to that, a further possibility might be to increase the S partial pressure by introducing more S into the synthesis to control the Ge and S volatility.

ACKNOWLEDGEMENTS

Financial supports gained from HZB Graduate School MatSEC (Materials for Solar Energy Conversion). Furthermore, the research leading to the presented results has been partially supported by the STARCELL project as well as INFINITE-CELL project. These projects have received funding from the European Union's Horizon 2020 research and innovation programme under the Marie Skłodowska-Curie grant agreements No 720907 and 777968 respectively. Furthermore, we thank René Gunder for the technical support at the scanning electron microscope to perform the EDX mappings.

REFERENCES

[1] Q. Guo, G.M. Ford, W.-C. Yang, C.J .Hages, H.W. Hillhouse, R. Agrawal, Enhancing the performance of CZTSSe solar cells with Ge alloying, Sol. Energy Mater. Sol. Cells 105 (2012) 132-136.

[2] C. P. Heinrich, T.W. Day, W.G. Zeier, G.J. Snyder, W. Tremel, Effect of isovalent substitution on the thermoelectric properties of the $Cu_2ZnGeSe_{4-x}S_x$ series of solid solutions, J. Am. Chem. Soc. 136 (2014) 442−448.

[3] S. Giraldo, M. Neuschitzer, T. Thersleff, S. López-Marino, Y. Sánchez, H. Xie, M. Colina, M. Placidi, P. Pistor, V. Izquierdo-Roca, K. Leifer, A. Pérez-Rodríguez, E. Saucedo, Large efficiency improvement in $Cu_2ZnSnSe_4$ solar cells by introducing a superficial Ge nanolayer, Adv. Energy Mater. 5 (2015) 1501070.

[4] T. Maeda, A. Kawabata, T. Wada, First-principles study on alkali-metal effect of Li, Na and K in Cu_2ZnGeS_4 and $Cu_2ZnGeSe_4$, Phys. Status Solidi (c) 12 (6) (2015) 631–637.

[5] A. Mule, B. Vermang, M. Sylvester, G. Brammertz, S. Ranjbar, T. Schnabel, N. Gampa, M. Meuris, J. Poortmans, Effect of different alkali (Li, Na, K, Rb, Cs) metals on $Cu_2ZnGeSe_4$ solar cells, Thin Solid Films 633 (2017) 156–16.

[6] Y.S. Lee, T. Gershon, O. Gunawan, T.K. Todorov, T. Gokmen, Y. Virgus, S. Guha, $Cu_2ZnGeSe_4$ thin-film solar cells by thermal co-evaporation with 11.6 % efficiency and improved minority carrier diffusion length, Adv. Energy Mater. 5 (2015) 1401372–1401375.

[7] T. Schnabel, M. Seboui, E. Ahlswede, Band gap tuning of $Cu_2ZnGeS_xSe_{4-x}$ absorbers for thin-film solar cells, Energies 10 (2017) 1813-1822.

[8] G. Gurieva, D.M. Többens, M. Ya. Valakh, S. Schorr, Cu-Zn disorder in $Cu_2ZnGeSe_4$, A complementary neutron diffraction and Raman spectroscopy study, J. Phys. Chem. Solids 99 (2016) 100-104.

[9] R. Gunder, J.A. Márquez-Prieto, G. Gurieva, T. Unold, S. Schorr, Structural characterization of off-stoichiometric kesterite-type $Cu_2ZnGeSe_4$ compound semiconductors: from cation distribution to intrinsic point defect density, CrystEngComm 20 (2018) 1465–1604.

[10] S. Chen, A. Walsh, Y. Luo, J.H. Yang, X.G. Gong, S.H. Wei, Wurtzite-derived polytypes of kesterite and stannite quaternary chalcogenide semiconductors, Phys. Rev. B: Condens. Matter 82 (2010) 195203-195211.

[11] K. Doverspike, K. Dwight, A. Wold, Preparation and characterization of $Cu_2ZnGeS_{4-y}Se_y$, Chem. Mater. 2 (2) (1990) 194-197.

[12] O.V. Parasyuk, L.V. Piskach, Y.E. Romanyuk, I.D. Olekseyuk, V.I. Zaremba, V.I. Pekhnyo, Phase relations in the quasi-binary Cu_2GeS_3-ZnS and quasi-ternary Cu_2S-Zn(Cd)S-GeS_2 systems and crystal structure of Cu_2ZnGeS_4, J. Alloys Compd. 397 (2005) 85–94.

[13] O.V. Parasyuk, L.D. Gulay, Y.E. Romanyuk, L.V. Piskach, Phase diagram of the Cu_2GeSe_3-ZnSe system and crystal structure of the $Cu_2ZnGeSe_4$ compound, J. Alloys Compd. 329 (2001) 202–207.

[14] S.M. Bagheri, I.J. Alverdijev, S.Z. Imamaliyeva, M.B. Babanly, The phase equilibria in the Cu_8GeS_6-Cu_8GeSe_6 system and thermodynamic properties of solid solutions, Chem. J. 4 (2) (2014) 26-31.

[15] M. Ishii, M. Onoda, K. Shibata, Structure and vibrational spectra of argyrodite family compounds Cu_8SiX_6 (X = S, Se) and Cu_8GeS_6, Solid State Ionics 121 (1999) 11-18.

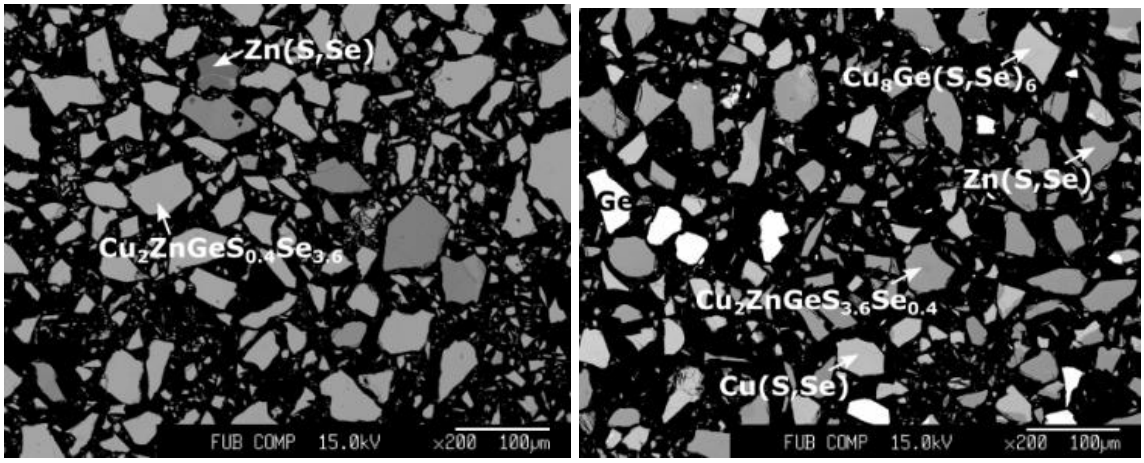

Fig. 1. BSE image of (left) $Cu_2ZnGeS_{0.4}Se_{3.6}$ (intended composition): grey - $Cu_2ZnGeS_{0.4}Se_{3.6}$ (intended composition), dark grey - Zn(Se,S), black - epoxy matrix) and (right) $Cu_2ZnGeS_{3.6}Se_{0.4}$ (intended composition): grey - $Cu_2ZnGeS_{3.6}Se_{0.4}$ (intended composition), dark grey - Zn(S,eS), light grey - $Cu_8Ge(S,Se)_6$, very light grey - Cu(S,Se) white - Ge, black - epoxy matrix).

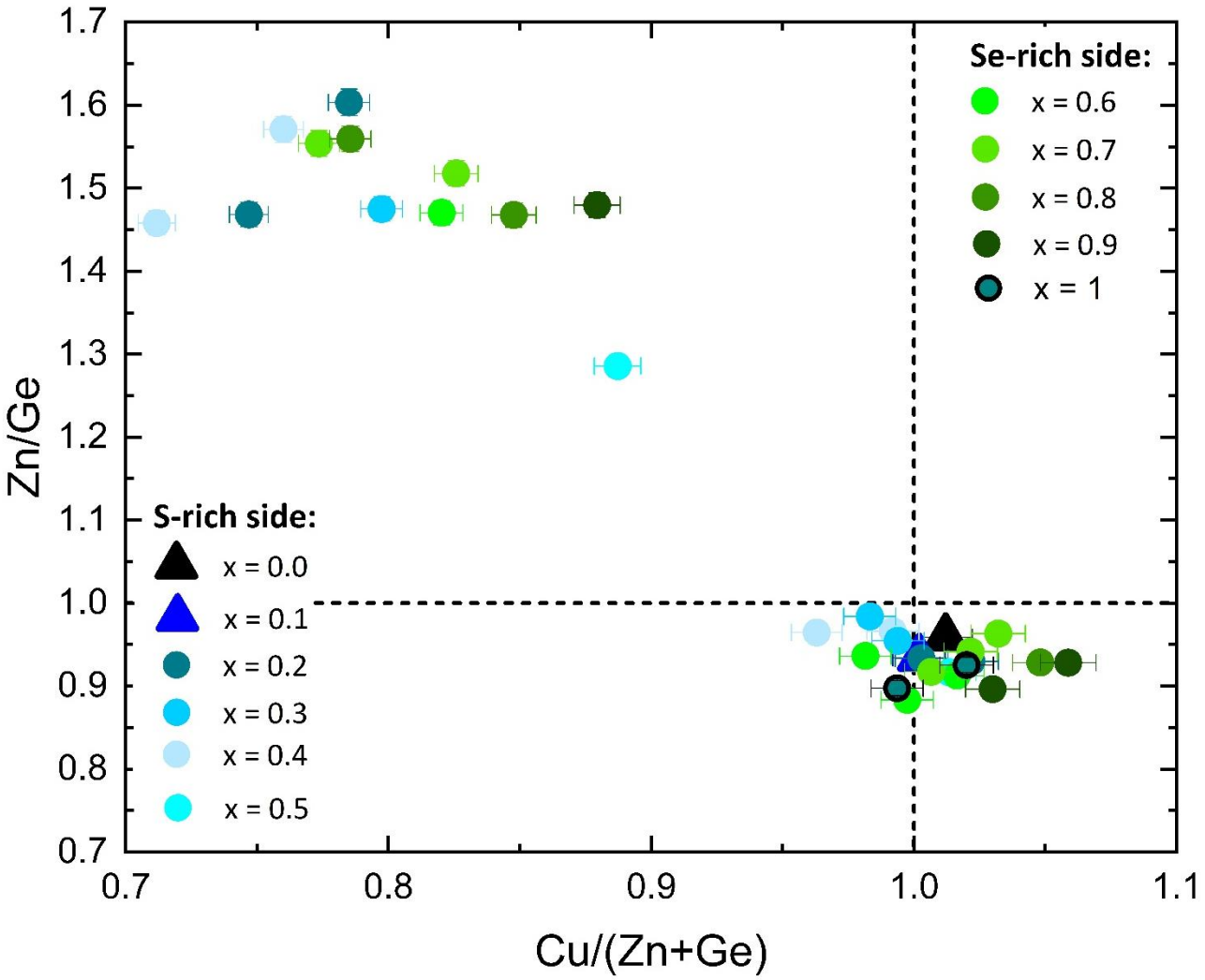

Fig. 2. Cation ratio plot Cu/(Zn+Ge) vs. Zn/Ge showing the off-stoichoimetry and the number of quaternary phases within the samples of the solid solution. Triangles show the single quaternary phases, whereas the dots indicate multiple quaternary phases within one sample. In the legend the intended instead of the real composition of the anion ratios is listed, due to the fact that different anion ratios are realized within one sample since more quaternary phases are present in one sample.

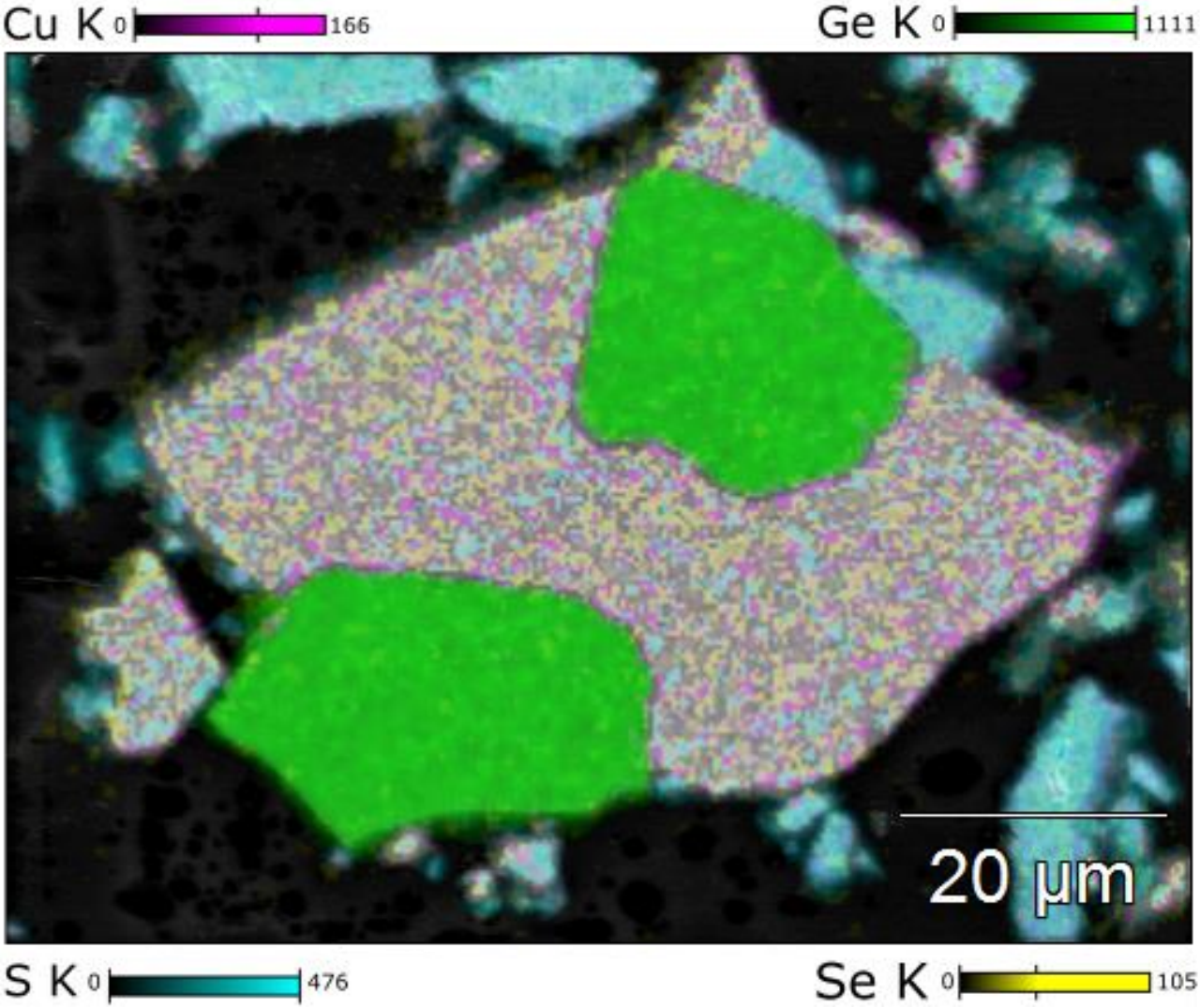

Fig. 3. EDX image of $Cu_2ZnGeS_{0.4}Se_{3.6}$ (intended composition) shows the elemental distribution of an intergrowth of Cu(S,Se) and Ge as secondary phases.

Table 1
Temperature program used for the synthesis of polycrystalline $Cu_2ZnGe(S_{1-x}Se_x)_4$ powder samples.

Step	**Stage**	**heating rate [K/h]**	**T [°C]**	**T_{hold} [h]**
1st reaction step	1st heating stage	10	250	48
	2nd heating stage	10	450	48
	3rd heating stage	10	650	48
	final heating stage	10	700-750	300
	cooling	10	RT	
homogenization		grinding of material and pressing to pellets		
2nd reaction step	1st heating stage	10	700-750	300
	cooling	10	RT	

Table 2
Chemical compositions of the quaternary phases of each polycrystalline powder sample of $Cu_2ZnGe(S_{1-x}Se_x)_4$ and secondary phases analyzed by WDX.

	Cu/(Zn+Ge)	Zn/Ge	S/(S+Se)	secondary phases
x = 0	1.012	0.959	1.0	ZnS; Cu_2S
x = 0.1	1.002	0.934	0.954	Zn(S,Se); Cu(S,Se); $Cu_8Ge(S,Se)_6$; Ge
x = 0.2	1.003	0.934	0.835	Zn(S,Se)
	1.022	0.930	0.854	Ge
	0.747	1.468	0.892	
	0.785	1.603	0.766	
x = 0.3	0.992	0.966	0.841	Zn(S,Se),
	0.963	0.964	0.836	Cu(S,Se)
	0.760	1.571	0.763	$Cu_8Ge(S,Se)_6$
	0.712	1.458	0.765	Ge
x = 0.4	0.983	0.984	0.649	Zn(S,Se)
	0.994	0.954	0.651	Cu(S,Se)
	0.797	1.475	0.585	$Cu_8Ge(S,Se)_6$
x = 0.5	1.013	0.917	0.514	Cu(S,Se)
	0.887	1.286	0.530	
x = 0.6	1.016	0.913	0.402	Zn(S,Se)
	0.997	0.833	0.404	
	0.982	0.936	0.415	
	0.820	1.471	0.308	
x = 0.7	0.774	1.554	0.323	Zn(S,Se)
	0.826	1.518	0.316	$Cu_8Ge(S,Se)_6$
	1.007	0.917	0.409	
	1.032	0.963	0.392	
	1.022	0.942	0.390	
x = 0.8	1.048	0.928	0.228	Zn(S,Se)
	0.848	1.468	0.192	$Cu_8Ge(S,Se)_6$
	0.785	1.559	0.188	
x = 0.9	0.879	1.480	0.097	Zn(S,Se)
	1.059	0.928	0.109	
	1.030	0.896	0.109	
x = 1	1.020	0.925	0	ZnSe
	0.994	0.897	0	